Article

Simulations of DNA Pol R517 Mutants Indicate 517's Crucial Role in Ternary Complex Stability and Suggest DNA Slippage Origin

Meredith C. Foley, and Tamar Schlick

J. Am. Chem. Soc., **2008**, 130 (12), 3967-3977 • DOI: 10.1021/ja077982t

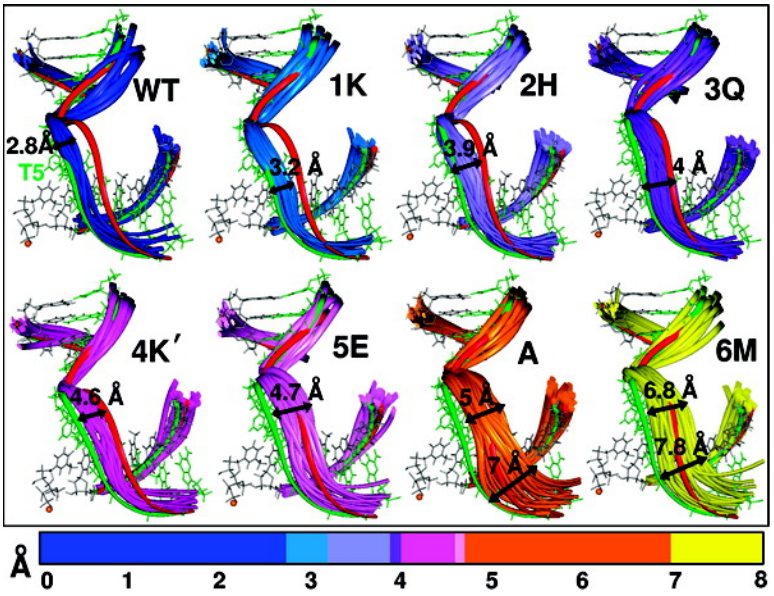

More About This Article

Additional resources and features associated with this article are available within the HTML version:

- Supporting Information
- Access to high resolution figures
- Links to articles and content related to this article
- Copyright permission to reproduce figures and/or text from this article

View the Full Text HTML

J|A|C|S
ARTICLES
Published on Web 02/29/2008

Simulations of DNA Pol λ R517 Mutants Indicate 517's Crucial Role in Ternary Complex Stability and Suggest DNA Slippage Origin

Meredith C. Foley and Tamar Schlick*

Department of Chemistry and Courant Institute of Mathematical Sciences, New York University, 251 Mercer Street, New York, New York 10012

Received October 21, 2007; E-mail: schlick@nyu.edu

Abstract: Unlike some other DNA polymerases, DNA polymerase λ (pol λ) utilizes DNA motion and active-site protein residue rearrangements rather than large-scale protein subdomain changes to transition between its active and inactive states. Pol λ also has an unusual error tendency to generate single-base deletions (also known as frameshift mutations) resulting from DNA template-strand slippage. An understanding of these features requires an atomic-level link between the various structures and motions involved and observed in biochemical functions. Our simulations of pol λ ternary complexes of various 517 mutants (Lys, Glu, His, Met, and Gln) reveal discrete orientations of the 517 residue with respect to the DNA and associated interactions (mainly electrostatic) that explain the wide range (∼3−8 Å) of mutant-dependent DNA motion observed (Figure 2 of manuscript): (wild-type < [R517K ∼ R517H ∼ R517Q] < [R517E ∼ R517A ∼ R517M]). This motion critically impacts stability of the ternary complex and hence drives/hampers the enzyme's catalytic cycle. In addition to pinpointing a trend for interpreting associated frameshift error rates based on template-strand stability, the close connection between DNA movement and active-site protein residue changes suggests that pol λ's unique architecture facilitates frameshift errors because small variations in the active-site environment (e.g., orientation of 517) can have large effects on the dynamics of the ternary pol λ complex.

1 Introduction

One of the challenges in the field of DNA repair is to interpret DNA polymerase mechanisms, in particular fidelity behavior, at atomic resolution. These enzymes are responsible for preserving the genetic integrity of a cell during DNA replication and repair. Although all polymerases have a similar structure likened to a hand with fingers, a palm, and a thumb,[1] they perform their designated tasks with varying levels of accuracy.[2] Numerous human diseases have been associated with DNA polymerase errors.[3,4] Thus, research on DNA polymerase fidelity could ultimately contribute to a better understanding of cancer, aging, and many neurodegenerative diseases that result from polymerase errors.

DNA polymerase λ (pol λ), a member of the DNA polymerase X family, poses intriguing questions due to its significant DNA motion during catalytic cycling and unusual error specificity − it makes many more frameshift errors through single-base deletions than base-substitution errors.[5] Like other members of the X family, pol λ's principal activity is to repair small damaged areas of DNA,[6] specifically within the base excision repair[7−11] and nonhomologous end joining[12−16] pathways. Although pol λ's base-substitution fidelity, 10^{-4}−10^{-5}, is similar to that of related DNA polymerase β (pol β),[17] its unique properties suggest an alternate fidelity mechanism. These differences include a higher deletion error rate for pol λ than that of pol β, a lack of large-scale protein motion in its catalytic cycle, and weak protein/DNA interactions compared to those of pol β.

(1) Steitz, T. A. *J. Biol. Chem.* **1999**, *274*, 17395−17398.
(2) Rothwell, P. J.; Waksman, G. *Adv. Protein Chem.* **2005**, *71*, 401−440.
(3) Kunkel, T. A. *Cancer Cell* **2003**, *3*, 105−110.
(4) Sweasy, J. B.; Lauper, J. M.; Eckert, K. A. *Radiat. Res.* **2006**, *166*, 693−714.
(5) Bebenek, K.; Garcia-Diaz, M.; Blanco, L.; Kunkel, T. A. *J. Biol. Chem.* **2003**, *278*, 34685−34690.
(6) Moon, A. F.; Garcia-Diaz, M.; Batra, V. K.; Beard, W. A.; Bebenek, K.; Kunkel, T. A.;Wilson, S. H.; Pedersen, L. C. *DNA Repair* **2007**, *6*, 1709−1725.
(7) Garcia-Diaz, M.; Bebenek, K.; Kunkel, T. A.; Blanco, L. *J. Biol. Chem.* **2001**, *276*, 34659−34663.
(8) Braithwaite, E. K.; Prasad, R.; Shock, D. D.; Hou, E. W.; Beard, W. A.; Wilson, S. H. *J. Biol. Chem.* **2005**, *280*, 18469−18475.
(9) Braithwaite, E. K.; Kedar, P. S.; Lan, L.; Polosina, Y. Y.; Asagoshi, K.; Poltoratsky, V. P.; Horton, J. K.; Miller, H.; Teebor, G. W.; Yasui, A.; Wilson, S. H. *J. Biol. Chem.* **2005**, *280*, 31641−31647.
(10) Lebedeva, N. A.; Rechkunova, N. I.; Dezhurov, S. V.; Khodyreva, S. N.; Favre, A.; Blanco, L.; Lavrik, O. I. *Biochim. Biophys. Acta* **2005**, *1751*, 150−158.
(11) Tano, K.; Nakamura, J.; Asagoshi, K.; Arakawa, H.; Sonoda, E.; Braithwaite, E. K.; Prasad, R.; Buerstedde, J.-M.; Takeda, S.; Watanabe, M.; Wilson, S. H. *DNA Repair* **2007**, *6*, 869−875.
(12) Lee, J. W.; Blanco, L.; Zhou, T.; Garcia-Diaz, M.; Bebenek, K.; Kunkel, T. A.; Wang, Z.; Povirk, L. F. *J. Biol. Chem.* **2004**, *279*, 805−811.
(13) Fan, W.; Wu, X. *Biochem. Biophys. Res. Commun.* **2004**, *323*, 1328−1333.
(14) Ma, Y.; Lu, H.; Tippin, B.; Goodman, M. F.; Shimazaki, N.; Koiwai, O.; Hsieh, C.-L.; Schwarz, K.; Lieber, M. R. *Mol. Cell* **2004**, *16*, 701−713.
(15) Nick McElhinny, S. A.; Havener, J. M.; Garcia-Diaz, M.; Juarez, R.; Bebenek, K.; Kee, B. L.; Blanco, L.; Kunkel, T. A.; Ramsden, D. A. *Mol. Cell* **2005**, *19*, 357−366.
(16) Capp, J.-P.; Boudsocq, F.; Bertrand, P.; Laroche-Clary, A.; Pourquier, P.; Lopez, B. S.; Cazaux, C.; Hoffmann, J.-S.; Canitrot, Y. *Nucleic Acids Res.* **2006**, *34*, 2998−3007.
(17) Fiala, K. A.; Duym, W. W.; Zhang, J.; Suo, Z. *J. Biol. Chem.* **2006**, *281*, 19038−19044.

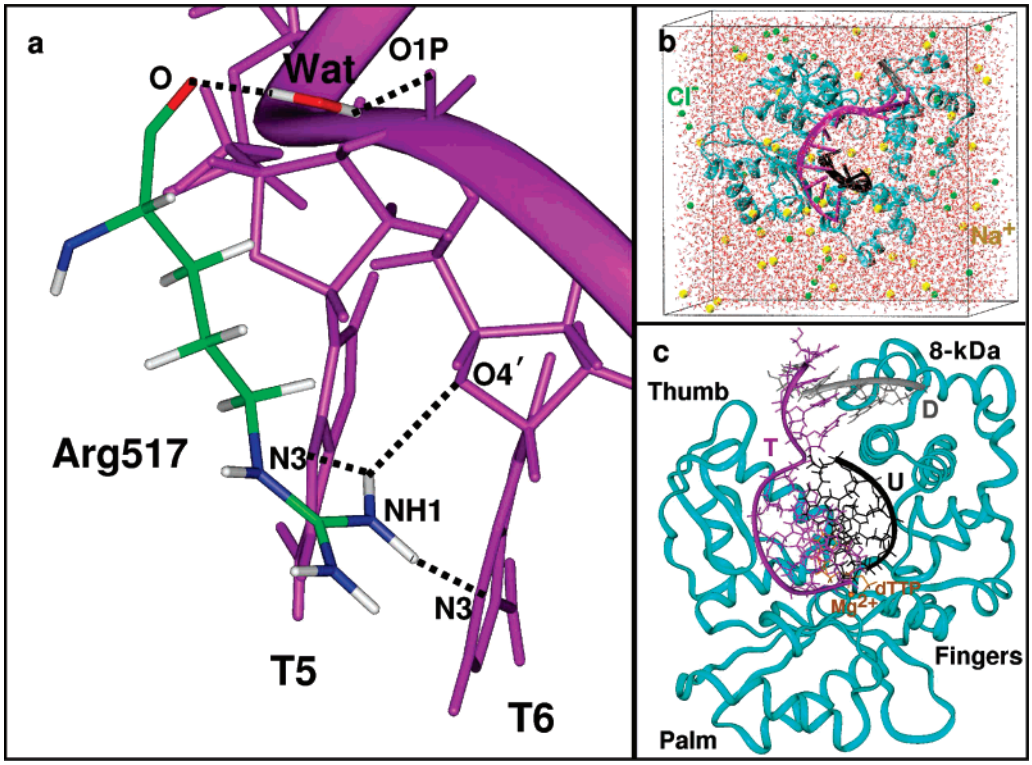

Figure 1. Pol λ/DNA/dTTP ternary system and Arg517's interactions with the DNA. T5, templating base at the gap; T6, adjacent template base that pairs with the primer terminus; Wat, a water molecule; T, DNA template strand; D, DNA downstream primer; U, DNA upstream primer. Dashed lines indicate hydrogen bonds.

Undoubtedly, polymerase-specific protein/DNA interactions and motions account in part for these differences. To interpret pol λ's distinct error profile, we perform molecular dynamics simulations to elucidate the atomic-level details involved in these interactions and motions.

Pol λ's architecture (Figure 1)[1] has been revealed by a series of pioneering X-ray crystal structures.[18−23] In addition to the typical hand domain, pol λ has an 8 kDa domain, an N-terminal BRCT domain,[24,25] and a serine−proline-rich linker region connecting the BRCT and 8 kDa domains.

These crystal structures involve the binary state (i.e., pol λ complexes with DNA before chemistry) and the ternary state (i.e., pol λ bound to the DNA and correct dNTP; dNTP: 2′-deoxynucleotide triphosphate) and provide several snapshots of pol λ complexes during the catalytic pathway for single-nucleotide gap filling.[19] They suggest steps in pol λ's fidelity mechanism where a key conformational rearrangement is a repositioning of the DNA template strand with an approximately 5 Å shift; this change repositions the templating base at the gap into a more favorable catalytic position, allowing it to basepair with an incoming dNTP. Our simulations are designed to provide a dynamic representation of these movements to elucidate the changes occurring at the atomic level.

Here we continue to investigate pol λ's dynamics/functional relationship by following leads that emerged in our previous study, which investigated pol λ's conformational transitions before correct dNTP incorporation[26] and revealed a series of concerted side-chain motions. Specifically, our prior wild-type simulations of the ternary pol λ complex suggested that Arg517 is crucial for constraining the system with bound substrate (dNTP) because of key Arg517/templating base interactions; our simulation of the Arg517Ala pol λ mutant ternary complex[26] also suggested an important role for Arg517 in maintaining the position of the DNA in the ternary conformation because the DNA moved back and forth between the ternary and binary positions in the Ala mutant system. This captured behavior is significant because it preceded experiments that revealed the dual conformation of the template strand in the recently crystallized Arg517Ala pol λ mutant.[23]

An examination of the wild-type X-ray crystal structure[19] and our previous simulations of wild-type pol λ[26] show that, in the ternary state of pol λ, Arg517 assumes a position similar to pol β's base-checking residue, Arg283, in pol β's closed state. Figure 1 shows some of the hydrogen-bonding possibilities between the Arg517 side chain and the DNA in pol λ's ternary state as deduced from our previous work. This fact again reinforces the potential crucial role of Arg517 in pol λ, because Arg283 in pol β critically affects fidelity.[27−31]

(18) Garcia-Diaz, M.; Bebenek, K.; Krahn, J. M.; Blanco, L.; Kunkel, T. A.; Pedersen, L. C. *Mol. Cell* **2004**, *13*, 561−572.
(19) Garcia-Diaz, M.; Bebenek, K.; Krahn, J. M.; Kunkel, T. A.; Pedersen, L. C. *Nat. Struct. Mol. Biol.* **2005**, *12*, 97−98.
(20) Garcia-Diaz, M.; Bebenek, K.; Krahn, J. M.; Pedersen, L. C.; Kunkel, T. A. *Cell* **2006**, *124*, 331−342.
(21) Picher, A. J.; Garcia-Diaz, M.; Bebenek, K.; Pedersen, L. C.; Kunkel, T. A. *Nucleic Acids Res.* **2006**, *34*, 3259−3266.
(22) Garcia-Diaz, M.; Bebenek, K.; Krahn, J. M.; Pedersen, L. C.; Kunkel, T. A. *DNA Repair* **2007**, *6*, 1333−1340.
(23) Bebenek, K.; Garcia-Diaz, M.; Foley, M. C.; Pedersen, L. C.; Schlick, T.; Kunkel, T. A. Substrate-Induced DNA Strand Misalignment During Catalytic Cycling by DNA Polymerase λ *EMBO Reports* **2008**, in press.
(24) Callebaut, I.; Mornon, J. *FEBS Lett.* **1997**, *400*, 25−30.
(25) Bork, P.; Hofmann, K.; Bucher, P.; Neuwald, A. F.; Altschul, S. F.; Koonin, E. V. *FASEB J.* **1997**, *11*, 68−76.
(26) Foley, M. C.; Arora, K.; Schlick, T. *Biophys. J.* **2006**, *91*, 3182−3195.
(27) Beard, W. A.; Osheroff, W. P.; Prasad, R.; Sawaya, M. R.; Jaju, M.; Wood, T. G.; Kraut, J.; Kunkel, T. A.; Wilson, S. H. *J. Biol. Chem.* **1996**, *271*, 12141−12144.

Recently, the hypothesis of a connection between Arg517/DNA interactions and template-strand slippage has been bolstered by deletion error data for Arg517Lys and Arg517Ala pol λ mutants. These revealed that mutants generate 3.3-fold and 3.7-fold greater single-base deletions, respectively, than wild-type pol λ.[23] This was not expected, because lysine, like arginine, is a basic residue. Although the accuracy of MD simulations is not sufficient to explain a small quantitative difference in error rates as found between the Lys and Ala mutants, state-of-the-art force fields and simulation protocols can provide insights into the atomic-level behavior of protein/DNA interactions to interpret, and possibly predict, qualitative differences in DNA template-strand slippage behavior. Indeed, when crystal structures are interpreted in tandem with MD simulation data, unexpected features sometimes emerge. The dual conformations of the template strand (corresponding to the binary and ternary positions) exhibited in an X-ray structure of the Arg517Ala pol λ/DNA binary complex,[23] for example may be explained by the conformational heterogeneity occurring in our Arg517Ala mutant simulation.[26] These structures and simulations also led to our recent hypothesis[23] that pol λ's slippage tendency is caused by dNTP-induced conformational changes of the template strand that occur during the enzyme's catalytic cycling.

To explore further the specific error behavior of pol λ, we focus here on the role of Arg517 on pol λ's interactions and motions. Specifically, we test the hypothesis that specific interactions between Arg517 and the DNA may deter template-strand slippage in the ternary state. Our studies investigate several other 517 mutants, such as Arg517Glu, Arg517His, Arg517Met, and Arg517Gln, to elucidate systematically the effect of the size and charge of the residue at position 517 on each system's template DNA stability and associated motions. This information, combined with the experimental data and prior simulation data for Arg517Ala, Arg517Lys, and wild-type pol λ systems,[26,23] helps describe those interactions (e.g., hydrogen bonds and electrostatics) that promote DNA template-strand slippage in pol λ relative to other polymerases.

The present work goes beyond our previous findings:[26,23] we combine results from all of our 517 mutant simulations to identify systematic trends between DNA template-strand stability and pol λ's slippage tendency and analyze how specific protein/DNA hydrogen bonding and energetic interactions give rise to each trend. In particular, we find that the extent of DNA template-strand movement captured in the simulations is mutant dependent and mirrors the trends in frameshift error rates already determined for wild-type pol λ and the Lys and Ala mutants: wild-type < [Arg517Lys ∼ Arg517His ∼ Arg517Gln] < [Arg517Glu ∼ Arg517Ala ∼ Arg517Met]. These trends directly reflect the strength of hydrogen bonding interactions between residue 517 and the DNA: Arg in the wild-type enzyme forms the most interactions; Lys, His, and Gln form a few; and Glu, Ala, and Met only form a few unstable hydrogen bonds through water molecules.

Moreover, our simulations reveal that Lys517, Glu517, and Met517 can assume three distinct orientations with respect to the DNA, whereas His517 and Gln517 can assume two different orientations based on specific dihedral angles of their side chains; we term these positions as toward, away, and extremely away from the DNA. Importantly, these orientations dictate residue interactions with the DNA, with the toward orientation often providing the most favorable interactions. The marked structural and energetic differences for the mutant systems with respect to the wild-type enzyme help explain the increased DNA motion in the mutants and indicate how pol λ's stability depends critically on the highly conserved 517 residue. In turn, pol λ's slippage tendency can be explained by single-point mutations and any other factors (e.g., water and ions) that disturb the delicate stability of the ternary complex.

2. Computational Methods

2.1. Initial Models. Six initial models were prepared based on the crystal pol λ ternary (PDB entry 1XSN) complex. In two models, Arg517 is mutated to lysine and, in the remaining four models, Arg517 is mutated to glutamate, histidine, methionine, and glutamine, respectively. To investigate the effect of the catalytic ion, the catalytic ion was added to the active site in all models except one of the Arg517Lys pol λ models. It was positioned by superimposing the pol λ protein C_α atoms onto those of another pol λ ternary complex (PDB entry 2BCV) that contains a Na^+ in the catalytic ion position. The ion was then mutated to Mg^{2+}, the hypothesized species of the catalytic ion for DNA polymerases.

In the initial structures, missing protein residues 1−11 were added. An oxygen atom was added to the 3′ carbon of the ddTTP sugar moiety to form 2′-deoxythymidine 5′-triphosphate (dTTP). All other missing atoms from the X-ray crystal structure were also added to our models. Mutant residue Ala543 of the protein was also replaced with Cys543 to reflect the natural amino acid sequence.

Optimized periodic boundary conditions in a cubic cell were introduced to all complexes using the *PBCAID* program.[32] The smallest image distance between the solute, the protein complex, and the faces of the periodic cubic cell was 10 Å. To obtain a neutral system at an ionic strength of 150 mM, the electrostatic potential of all bulk water (TIP3 model) oxygen atoms was calculated using the Delphi package.[33] Those water oxygen atoms with minimal electrostatic potential were replaced with Na^+ and those with maximal electrostatic potential were replaced with Cl^-. All of the Na^+ and Cl^- ions were placed at least 8 Å away from both protein and DNA atoms and from each other.

As depicted in Figure 1, all of the initial models contain around 38 323 atoms, 278 crystallographically resolved water molecules from the binary complex, 10 481 bulk water molecules, Mg^{2+} ions, incoming nucleotide dTTP, and 41 Na^+ and 29 Cl^- counterions. The final dimensions of the box are: $72.61 \times 75.97 \times 70.91$ Å^3.

2.2. Minimization, Equilibration, and Dynamics Protocol. The six simulations performed are as summarized in Table 1. All of the systems had an incoming nucleotide bound. Systems 1−6 represent ternary Arg517Lys, Arg517His, Arg517Gln, Arg517Lys, Arg517Glu, and Arg517Met pol λ mutant systems, respectively. System 4 is the ternary Arg517Lys system with the nucleotide-binding ion only, whereas system 1 is the Arg517Lys system with both magnesium ions. Initial energy minimizations and equilibration simulations were performed using the *CHARMM* program[34] with the all-atom C26a2 force field.[35] First, each system was minimized with fixed positions for all

(28) Werneburg, B. G.; Ahn, J.; Zhong, X.; Hondal, R. J.; Kraynov, V. S.; Tsai, M.-D. *Biochemistry* **1996**, *35*, 7041−7050.
(29) Ahn, J.; Werneburg, B. G.; Tsai, M.-D. *Biochemistry* **1997**, *36*, 1100−1107.
(30) Osheroff, W. P.; Beard, W. A.;Wilson, S. H.; Kunkel, T. A. *J. Biol. Chem.* **1999**, *274*, 20749−20752.
(31) Osheroff, W. P.; Beard, W. A.; Yin, S.; Wilson, S. H.; Kunkel, T. A. *J. Biol. Chem.* **2000**, *275*, 28033−28038.
(32) Qian, X.; Strahs, D.; Schlick, T. *J. Comput. Chem.* **2001**, *22*, 1843−1850.
(33) Klapper, I.; Hagstrom, R.; Fine, R.; Sharp, K.; Honig, B. *Proteins* **1986**, *1*, 47−59.
(34) Brooks, B. R.; Bruccoleri, R. E.; Olafson, B. D.; States, D. J.; Swaminathan, S.; Karplus, M. *J. Comput. Chem.* **1983**, *4*, 187−217.
(35) MacKerell, A., Jr.; Banavali, N. K. *J. Comput. Chem.* **2000**, *21*, 105−120.

Table 1. Summary of Simulations Performed before Chemistry[a]

simulation label	system	magnesium ions in active site
1K	ternary R517K	nuc + cat
2H	ternary R517H	nuc + cat
3Q	ternary R517Q	nuc + cat
4K′	ternary R517K	nuc
5E	ternary R517E	nuc + cat
6M	ternary R517M	nuc + cat

[a] nuc: nucleotide-binding ion; cat: catalytic ion.

heavy atoms except those from the added residues using SD for 5 000 steps followed by ABNR for 10 000 steps. Two cycles of further minimization were carried out for 10 000 steps using SD followed by 20 000 steps of ABNR. During minimization, all of the atoms except those of Cl^-, Na^+, and water were kept fixed, allowing the water molecules to relax around the protein/DNA complex. The equilibration process was started with a 30 ps simulation at 300 K using single-time step Langevin dynamics and keeping the constraints used in the previous minimization step. The SHAKE algorithm was employed to constrain the bonds involving hydrogen atoms. This was followed by unconstrained minimization using 10 000 steps of SD followed by 20 000 steps of ABNR. A further 30 ps of equilibration at 300 K and minimization consisting of 2000 steps of SD followed by 4000 steps of ABNR were performed. The final equilibration step involved 130 ps dynamics at 300 K. At the end of the equilibration phase, the protein and DNA remain similar to their ternary state conformations but small deviations from the ternary crystal complex occur as evidenced from the rmsd of the DNA not being equal to zero at the start of each simulation in Figure 3.

Production dynamics were performed using the program *NAMD*[36] with the *CHARMM* force field.[35] First, the energy in each system was minimized with fixed positions for all protein and DNA heavy atoms using the Powell algorithm. Systems were then equilibrated for 100 ps at constant pressure and temperature. Pressure was maintained at 1 atm using the Langevin piston method,[37] with a piston period of 100 fs, a damping time constant of 50 fs, and a piston temperature of 300 K. Temperature coupling was enforced by velocity reassignment every 2 ps. Then, production dynamics were performed at constant temperature and volume. The temperature was maintained at 300 K using weakly coupled Langevin dynamics of non-hydrogen atoms with damping coefficient $\gamma = 10$ ps^{-1} used for all simulations performed; bonds to all of the hydrogen atoms were kept rigid using SHAKE,[38] permitting a time step of 2 fs. The system was simulated in periodic boundary conditions, with full electrostatics computed using the PME method[39] with grid spacing on the order of 1 Å or less. Short-range nonbonded terms were evaluated at every step using a 12 Å cutoff for van der Waals interactions and a smooth switching function. The total simulation length for systems 1 and 4 was 20 ns and for systems 2, 3, 5, and 6 was 10 ns.

Simulations using the *NAMD* package were run on both local and NCSA SGI Altix 3700 Intel Itanium 2 processor shared-memory systems running the Linux operating system.

3. Results

3.1. DNA and Protein Subdomain Movement. Significantly, systematic mutant-dependent DNA motion is captured in all of our mutant simulations started from the ternary conformation, though no protein movement was observed; at the end of each simulation, the overall conformation of the protein is very similar to the crystal ternary conformation as shown in S1 (Supporting Information). Figure 2 reveals a remarkable range of DNA motion relative to the crystal binary and ternary positions that is mutant dependent. Interestingly, the largest motions are in the DNA template strand, whereas the primer fluctuates closely around its crystal position. In this figure and throughout, we denote the different mutant simulations as 1K, 2H, 3Q, 4K′, 5E, and 6M as in Table 1 for easy reference to the mutant type. The simulation index (1−6) reflects the extent of DNA motion in increasing order (Figure 2). Figure 3 shows corresponding rmsd plots of simulated DNA backbone atoms relative to those same atoms of the crystal binary and ternary complexes; the figures also provide comparative data for the Arg517Ala mutant and wild-type enzyme.[26] We see that the wild-type and Arg517Met mutant (6M) pol λ simulations represent opposite extremes of DNA motion, with the DNA staying very close to the crystal ternary position during the wild-type simulation and the DNA moving more than double, over a 7−8 Å range toward the binary position during the 6M simulation. This trend is also striking from Figure 3, where the rmsd for the ternary complex (green) steadily increases from a−h, whereas the value for the binary complex (red) decreases. In fact, each simulation displays a characteristic motion of the DNA template strand that directly reflects its DNA interactions with residue 517 (as we analyze in the next subsection). In increasing order of DNA motions, we have, wild-type < Lys (two ions bound) < His < Gln < Glu < Ala < Met, with corresponding ranges of motion as indicated in Figure 2.

In more detail, in simulations 1K and 2H, which display similar and slightly greater fluctuations of the DNA compared to the wild-type enzyme, the DNA remains in the ternary conformation throughout the simulation except for slight fluctuations toward the binary position. These involve only the DNA template strand backbone in simulation 1K (Figures 2 and 3) and somewhat further movement of the whole template strand in simulation 2H (Figures 2 and 3).

Larger DNA motions occur for the 3Q and 5E systems (Figures 2 and 3), with 3Q in the range of 2H (∼4 Å) and 5E in the range of the A mutant (∼5 Å).

In simulation 4K′, the DNA transits between the ternary and binary positions more frequently during the initial 13 ns (Figure 3). This motion mainly involves a change in the DNA template-strand backbone to an intermediate position between the binary and ternary positions (range of motion centered between the crystal states in Figure 2). The part of the DNA backbone that moves most frequently toward the binary position is the region above the template base at the gap, T5, and the two following bases, T6 and T7. This template triplet moves with the backbone motion, with T5 shifting the least, likely because of its constraint by interactions with Lys517 (below).

The longest and largest fluctuations occur for 6M (Figures 2 and 3).

3.2. Residue 517's Side-Chain Orientation and Hydrogen Bonding with the DNA. Our prior work suggested that Arg517 is essential for maintaining the position of the templating base at the gap in the ternary state and showed that it can form several hydrogen bonds with the DNA as seen in Figure 1.[26] The 517 mutant studies indicate that residue 517's side-chain orientation

(36) Phillips, J. C.; Braun, R.; Wang, W.; Gumbart, J.; Tajkhorshid, E.; Villa, E.; Chipot, C.; Skeel, R. D.; Kale, L.; Schulten, K. Scalable molecular dynamics with NAMD. *J. Comput. Chem.* **2005**, *26*, 1781−1802.
(37) Feller, S. E.; Zhang, Y.; Pastor, R. W.; Brooks, B. R. *J. Chem. Phys.* **1995**, *103*, 4613−4621.
(38) Ryckaert, J.-P.; Ciccotti, G.; Berendsen, H. J. C. *J. Comput. Phys.* **1977**, *23*, 327−341.
(39) Darden, T. A.; York, D. M.; Pedersen, L. G. *J. Chem. Phys.* **1993**, *98*, 10089−10092.

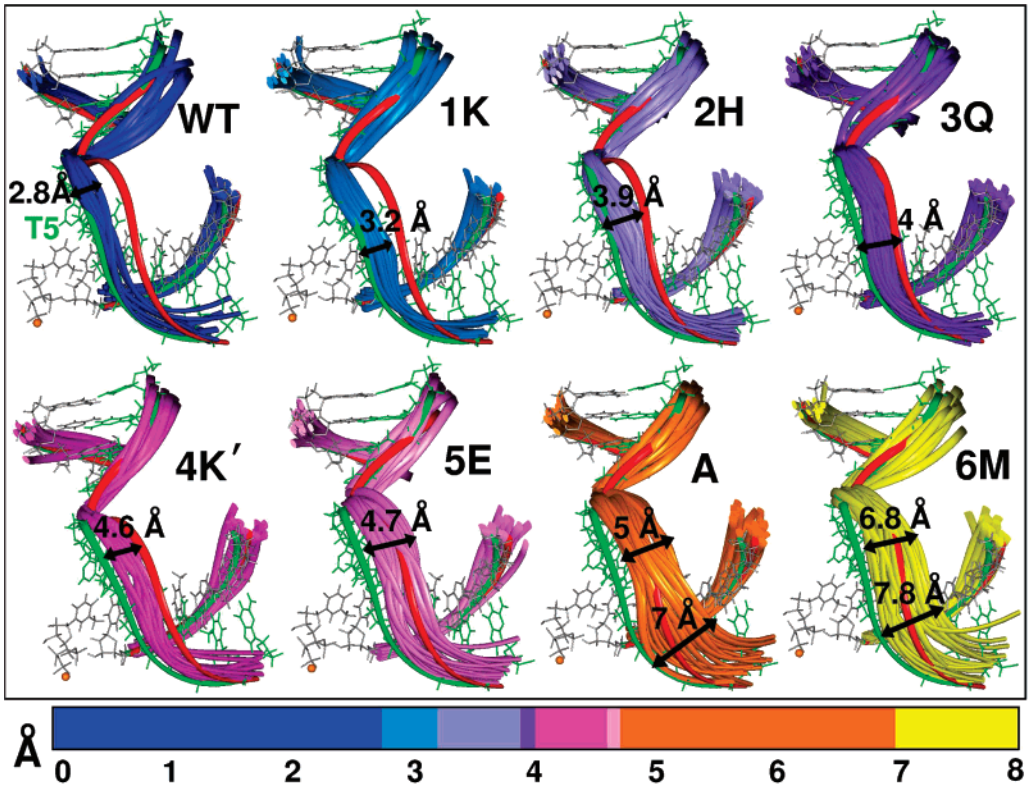

Figure 2. Ranges of DNA motion occurring in each 517 mutant simulation as well as in the wild-type (WT) simulation with the nucleotide-binding ion. Positions of the DNA are shown with reference to the crystal binary (red, PDB entry 1XSL) and ternary (green, PDB entry 1XSN) DNA positions. DNA bases of the template and primer strands are green and gray, respectively. A is the Arg517Ala pol λ mutant.

determines the hydrogen bonding with the DNA and that this, in turn, affects the stability of the DNA. Unlike Arg517, which assumes one steady orientation during simulations of wild-type pol λ,[26] the mutant residues undergo conformational changes that disrupt DNA interactions and result in increased DNA movement compared to wild-type pol λ.

Figure 4 shows the various orientations of the mutant residues captured during the simulations. Only Ala517 cannot assume multiple conformations because of its short side chain. The multiple conformations assumed by most of the mutants are probably explained by the inability of these residues to strongly interact with surrounding protein and DNA residues. Lys517 has one of the more flexible side chains and exhibits three distinct orientations based on these CG−CD−CE−NZ dihedral angle ranges: 60°, 200° and 300° (Figure 4); we term these Lys517 conformers as extremely away, toward, and away from the DNA, respectively, to indicate proximity to T5 (we similarly refer to all conformations of the other 517 residues). The 300° range or away conformation is similar to the orientation of Lys517 recently captured in the X-ray crystal structure of the Arg517Lys pol λ mutant.[23]

Glu517 and Met517 also exhibit three distinct side-chain conformations based on specific side-chain torsions as shown in Figure 4. Unlike Met517, which transitions quickly among all three conformers, Glu517 spends more time in one orientation (red a.k.a. extremely away orientation; Figure 4) because it is stabilized by interactions with nearby Ser526 and Leu527. His517 shows less conformational flexibility and switches between two orientations distinguished by the CA−CB−CG−ND1 dihedral angle (Figure 4). Gln517 adopts one steady orientation after it undergoes a conformational change at the beginning of the simulation (Figure 4).

Lys517, His517, and Gln517 show particular dependence on their side-chain orientation for hydrogen bonding with T5 and T6 as shown in Figures 5 and S2 (Supporting Information). Interestingly, these mutant simulations show among the least DNA movement toward the binary position (Figures 2 and 3). Only the Lys517 toward orientation supports steady hydrogen bonding with both T5:N3 and T6:N3, as shown in Figures 5 and S2 (Supporting Information), whereas hydrogen bonding with T6:O4′ does not appear to depend on a particular conformation of Lys517 (Figure S2, Supporting Information). Similarly, the toward (green, Figure 4) orientations of His517 and Gln517 support at least semistable hydrogen bonding with T5:N3 (Figure 5), whereas their alternative conformations do not. Ala517, Met517, and Glu517 do not directly hydrogen bond with the DNA.

Table 2 summarizes the hydrogen-bonding trends between residue 517 and the DNA in all of the simulations as well as prior wild-type pol λ/DNA and Ala mutant systems;[26] distance data for the wild-type enzyme used to construct Table 2 are given in Figure S3 (Supporting Information). All 517 mutant simulations show hydrogen bonding through water with the DNA backbone atom, T6:O1P, as shown in Figure 1. This hydrogen bond likely results from the stability of the DNA in the ternary orientation; for example, less DNA motion (e.g., in simulations 1K and 2H) corresponds to more frequent hydrogen bonding. Additional transient hydrogen bonding through waters occurs with T5 and T6 in the Lys, Glu, and Gln 517 mutant simulations (Tables 2 and S1 in the Supporting Information).

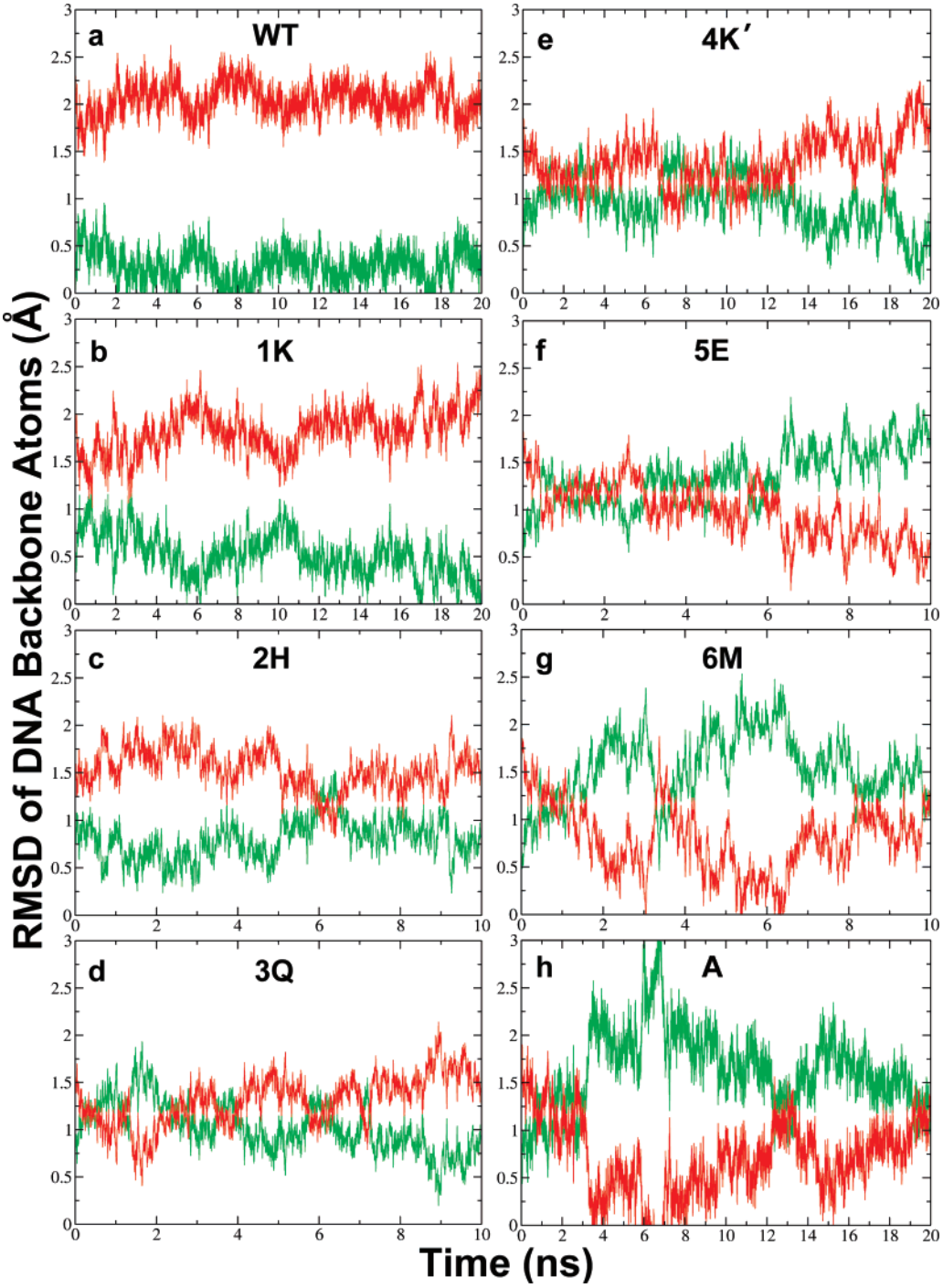

Figure 3. Time evolution of the rmsd of DNA backbone atoms (P, O3′, C3′, C4′, C5′, O5′, O5T) in all trajectories started from the ternary state (simulations 1K−6Q, wild-type, and R517A mutant) relative to the crystal binary (PDB entry 1XSL, red) and ternary (PDB entry 1XSN, green) structures. Superimposition is performed with respect to protein C_α atoms. rmsd plots do not start at zero because each system was equilibrated prior to production dynamics.

3.3. Interaction Energy between Residue 517 and the DNA. To assess in general terms the relative effects of van der Waals interactions and hydrogen bonding between each system's residue 517 and the DNA, we calculate interaction energies between each residue with T5 and T6 (Figure 6); note that a full treatment requires free-energy analysis. The systems used were the fully equilibrated systems of our wild-type, Arg517Ala, and Arg517Lys pol λ ternary models and the final states of our Arg517Lys, Arg517Glu, Arg517Gln, Arg517His, and Arg517Met mutant pol λ simulations. Recall that our equilibrated systems of both Arg517Lys pol λ models contain Lys517 in the toward orientation (dihedral conformers of 200°), while at the end of each 20 ns simulation the Lys517 side chain is in one of the away orientations (Figure 4).

Qualitatively, we see that Arg517 (wild-type 1 Mg and wild-type 2 Mg; Figure 6) has less electrostatic stabilization with T6 than T5, whereas van der Waals interactions with both bases are similar. With Ala517 (R517A 1 Mg; Figure 6), both electrostatic and van der Waals interactions decrease compared to wild-type Arg517. This was expected because Ala517 is much smaller than arginine and is neutrally charged.

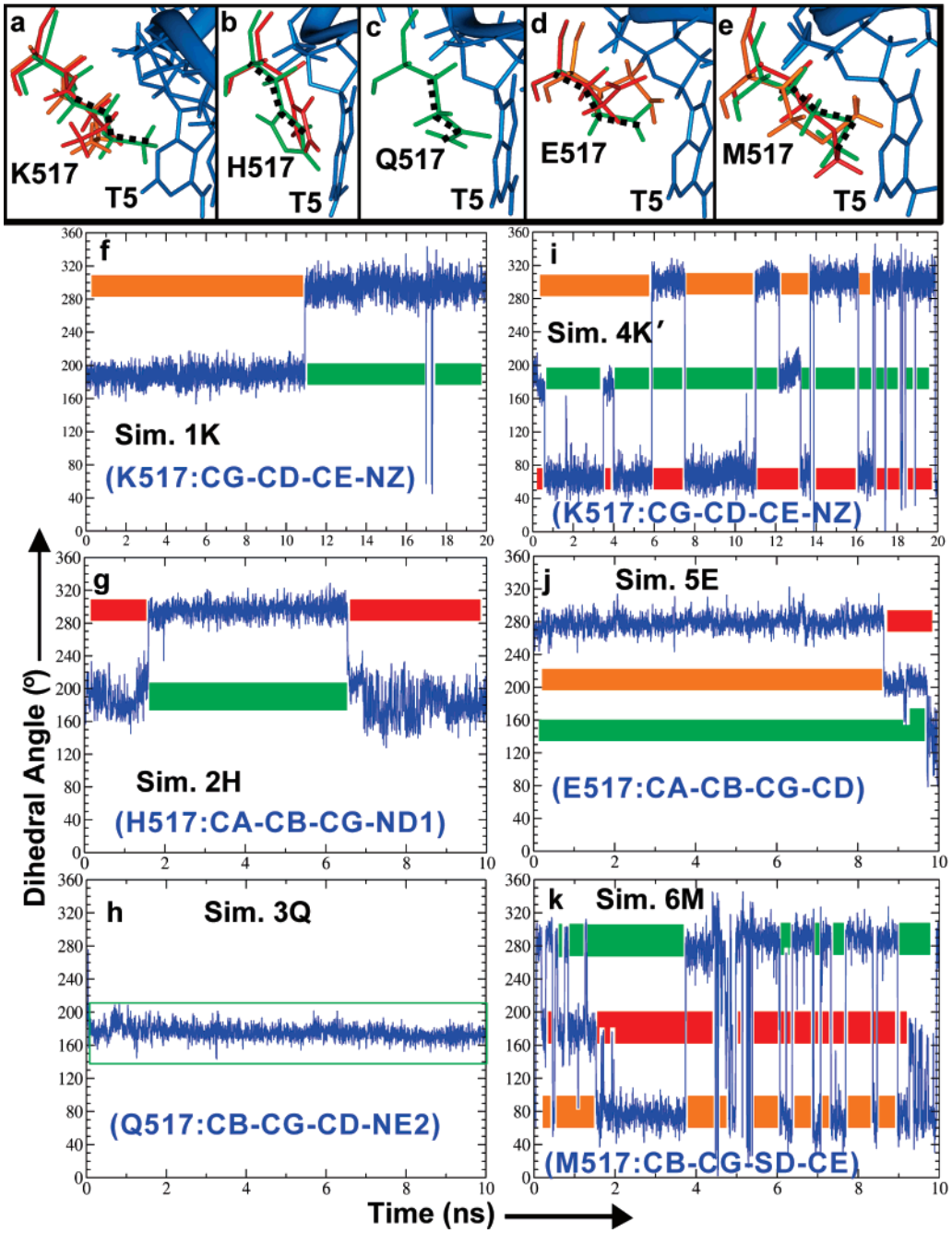

Figure 4. Time evolution of various 517 mutant side-chain dihedral angles and orientations representing three general conformational states: extremely away (red), toward (green), and away (orange) orientations, as discussed in the text. The dihedral angle used for each mutant is traced over the toward orientation with a dashed line in panels a−e.

Lys517 in the toward conformation (R517K 1 Mg toward and R517K 2 Mg toward, Figure 6) shows a greater DNA stability than can be attributed to the increased electrostatic interactions with T5 and T6, though van der Waals interactions somewhat decrease. When Lys517 is in the away conformation (R517K 2 Mg away, final state F; Figure 6), increased electrostatic and van der Waals interactions with T6 are realized, though at a cost of decreased interactions with T5. When Lys517 is in the extreme away orientation (R517K 1 Mg extreme away, F; Figure 6), van der Waals interactions with T5 and T6 similar to those in wild-type Arg517 occur but electrostatic interactions substantially decrease.

The importance of these electrostatic interactions on DNA stability is supported by the correlation between the orientation observations and movement toward the binary position. For the other residues, similar analyses apply, but fewer interactions with T6 than Lys517 or Arg517 occur due to their shorter side chains. Met and Glu have limited contacts with the DNA and have less favorable electrostatic interactions, whereas His and Gln have more favorable interactions but they are substantially less than Arg517.

In summary, our analysis suggests that both the length of the side chain at position 517 and its orientation significantly influence interactions with T5 and T6. More quantitative deductions require free-energy analysis.

3.4. The Effect of DNA Movement on Active-Site Organization. The mutant-dependent DNA motion also disrupts active-site organization by affecting primer terminus−dNTP

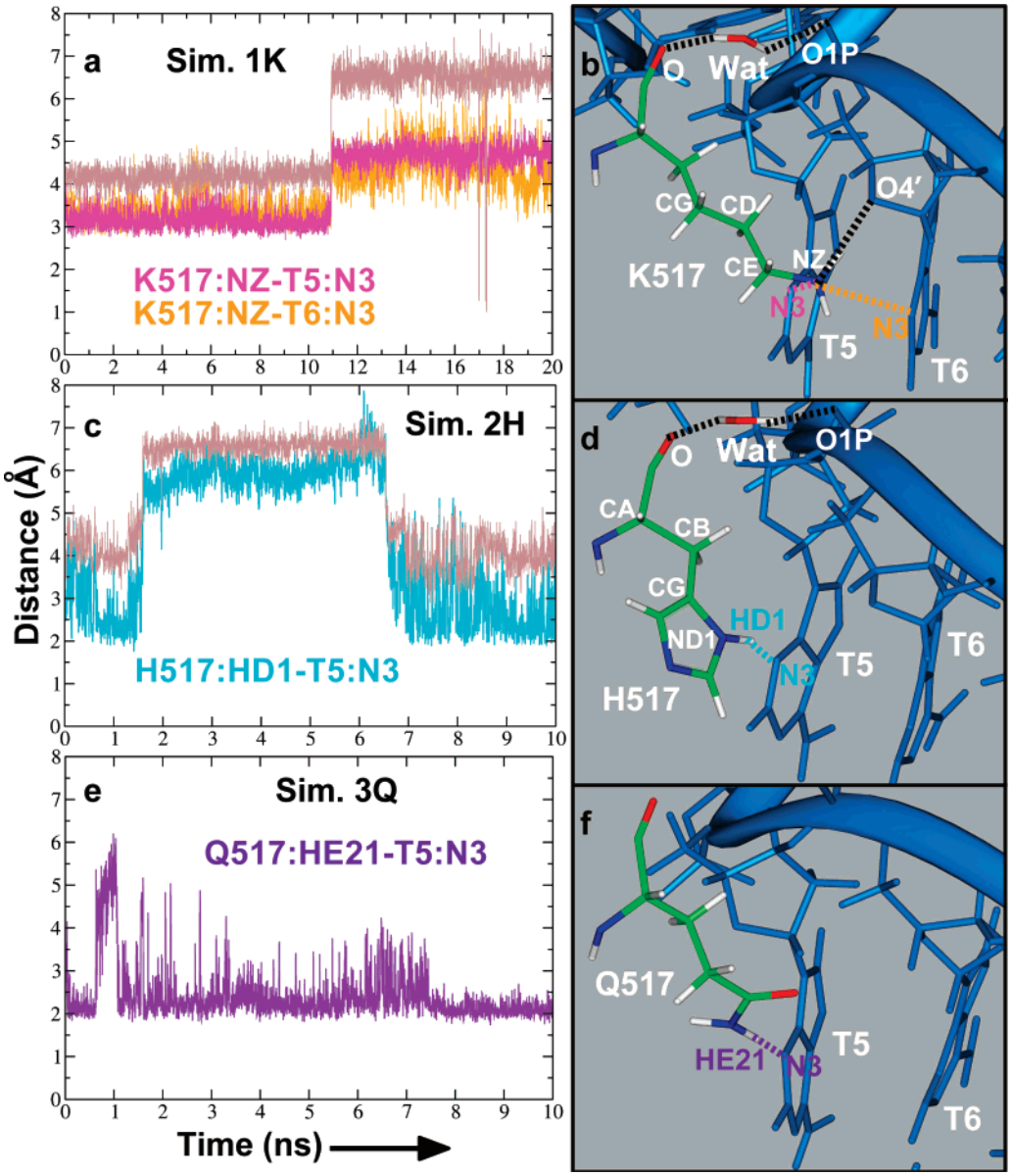

Figure 5. Stabilizing interactions between Lys517, His517, or Gln517 and nearby DNA bases, T5 and T6. The time evolution of key distances for simulations 1K, 2H, and 3Q are provided. Superimposed onto plots a and c are the K517:CG-CD-CE-NZ and H517:CA-CB-CG-ND1 dihedral angle plots (brown) from Figure 4, respectively, to reveal correlations in the data.

alignment and destabilizing several active-site residues (Ile492, Tyr505, and Phe506). The impact on active-site organization may be partially lessened, however, by the interactions of some residues (Arg488, Lys521, Lys544, and Arg538) with the DNA. Table 3 shows key active-site distances averaged over the simulation for all of the mutant systems. These simulations exhibit hexacoordination of the Mg^{2+} ions. Moreover, the nucleotide-binding ion is coordinated to one water molecule, Asp427, Asp429, and dTTP. The catalytic ion in simulations 1K−3Q and 5E−6M is coordinated to two water molecules and all three active-site aspartates (Asp427, Asp429, Asp490); this arrangement is similar to that determined in our wild-type ternary pol λ system with both ions.[26] The active-site distortion is most noticeable from the long average O3′−P_α distances in these simulations. The longest distance occurs in the Arg517Met mutant and likely results from the large DNA template strand motion. Mutants with shorter average distances (simulations 1K, 3Q, and 5E; Table 3) reflect the stabilization of the primer terminus by Arg488. This residue hydrogen bonds with a DNA backbone atom at the primer terminus, P6:O1P or O2P, as shown in Figures S4, S5, and S6 (Supporting Information). This may help to stabilize the primer terminus and align it with the incoming nucleotide when the catalytic ion is present to decrease the O3′−P_α distance.

Our previous study[26] revealed that, in transitioning from an inactive binary to an active ternary state upon binding the correct incoming nucleotide, pol λ undergoes: a movement of Arg514's side chain away from the binary-state position; a partial flip of Arg517 toward the ternary-state position; flips of Ile492, Phe506, and Tyr505 in succession until the DNA is fully positioned in the ternary conformation; and only then Arg514 and Arg517 complete their flips to their ternary-state positions. We hypothesize that these five residues act as gate-keepers, regulating the transition of the enzyme−substrate complex to a chemically competent state.

Table 2. Hydrogen Bonding between R517, K517, E517, H517, M517, Q517 or A517 and DNA

	DNA Atoms			
Simulation	T5:N3	T6:N3	T6:O4′	T6:O1P
1K	yes, with K517's ϵ-amino group over first 11 ns	yes, with K517's ϵ-amino group over first 11 ns	yes, with K517's ϵ-amino group	yes, through a water for 77% of simulation
2H	yes, with H517's HD1 for the first 2 ns and last 3 ns	no	no	yes, through a water for 67.1% of simulation
3Q	yes, with Q517's HE21	no	transiently, with Q517's OE1 through a water	transiently, through a water for 21.5% of simulation
4K′	rarely, with K517's ϵ-amino group	no	transiently, with K517's ϵ-amino group	transiently, through a water for 12.8% of simulation
5E	transiently, with E517's OE2 through a water	no	transiently, with E517's OE2 through a water	rarely, through a water for 3.2% of simulation
6M	no	no	no	transiently, through a water for 23.3% of simulation
ternary WT with dTTP and nuc bound[a]	yes, with an R517 NH1 hydrogen	yes, with an R517 NH1 hydrogen	yes, with an R517 NH1 hydrogen	yes, through a water for 78.8% of simulation
ternary WT with dTTP, nuc, and cat bound[a]	yes, with an R517 NH1 hydrogen	transiently, with an R517 NH1 hydrogen	transiently, with an R517 NH1 hydrogen	transiently, through a water for 33.5% of simulation
ternary R517A with dTTP and nuc bound[a]	no	no	no	rarely, through a water for 5.7% of simulation

[a] Simulations from ref 26; T5, template base at gap; T6, template base that pairs with the primer terminus; WT, wild-type; nuc, nucleotide-binding ion; cat, catalytic ion; dTTP, 2′-deoxythymidine 5′-triphosphate.

The movements of Ile492, Tyr505, and Phe506 in all of the simulations are summarized in Table S2 (Supporting Information). In each simulation, Tyr505 flips to its binary position but, in systems 2H, 3Q, and 6M, this occurs during the equilibration phase. The movement of Ile492 is more variable among the mutant simulations. Ile492 flips to its binary position in simulations 3Q, 6M, and our prior Ala mutant,[26] whereas it only temporary flips during simulation 1K. In the 4K′ system, Ile492 flips to the binary position during the equilibration phase but then changes orientation again to a position opposite to its ternary-state position during production dynamics. Ile492 also assumes this new position in simulation 5E. Only during simulation 4K′ does Phe506 flip to its binary position. The movements of these residues in our Arg517Lys pol λ systems (1K and 4K′) agree with the X-ray crystal structure of this mutant, which captures Ile492, Tyr505, and Phe506 in intermediate conformations close to those in the binary state.[23]

Working against these protein/DNA transitions are Lys521, Lys544, and Arg538, which form hydrogen bonds with the DNA template strand backbone in the ternary state. In all of the simulations, Lys521 hydrogen bonds with the DNA backbone at T4 and T6 (Figures S7, S8, and S9 in the Supporting Information). Lys544 and Arg538 occasionally hydrogen bond with the DNA backbone at T7 and T6, respectively, in simulations 3Q, 4K′, 5E, and 6M (Figures S7, S8, and S9 in the Supporting Information), and they steadily form hydrogen bonds in simulations 1K and 2H (Figures S7 and S8 in the Supporting Information).

4. Discussion

Our studies reveal that mutations of Arg517 significantly affect the stability of the DNA, though they do not induce subdomain conformational changes in the protein. The decreased stability is reflected by directed conformational sliding motions of the DNA that are mutant dependent, as evidenced by the dramatic trend of Figure 2. Although the DNA remains bound to pol λ, large rearrangements occur in the DNA template strand, whereas the primer remains close to its initial position. Decreased stability of the mutant complexes leads to the disassembly of the active site, which, in turn, likely explains in some cases (and predicts in others) a decrease in fidelity. Recent X-ray crystal structures of Ala and Lys pol λ mutants support this view as do experimental data showing that both the Arg517Lys and Arg517Ala mutants exhibit increased single-base deletions,[23] with the Arg517Ala pol λ mutant being the more error prone.

The combined theoretical and experimental data uncover a correlation between the DNA movement in the various pol λ systems and the known pattern of deletion errors (Figure 2): wild-type < [Arg517Lys ∼ Arg517His ∼ Arg517Gln] < [Arg517Glu ∼ Arg517Ala ∼ Arg517Met]. This correspondence supports the hypothesis that Arg517's interactions with the DNA stabilize the active site, resulting in a reduction of frameshift errors. At the same time, this explains why substituting other amino acids for Arg517, such as lysine or alanine, leads to a destabilization of the active site, sharply increasing pol λ's tendency for generating frameshift errors. Indeed, our simula-

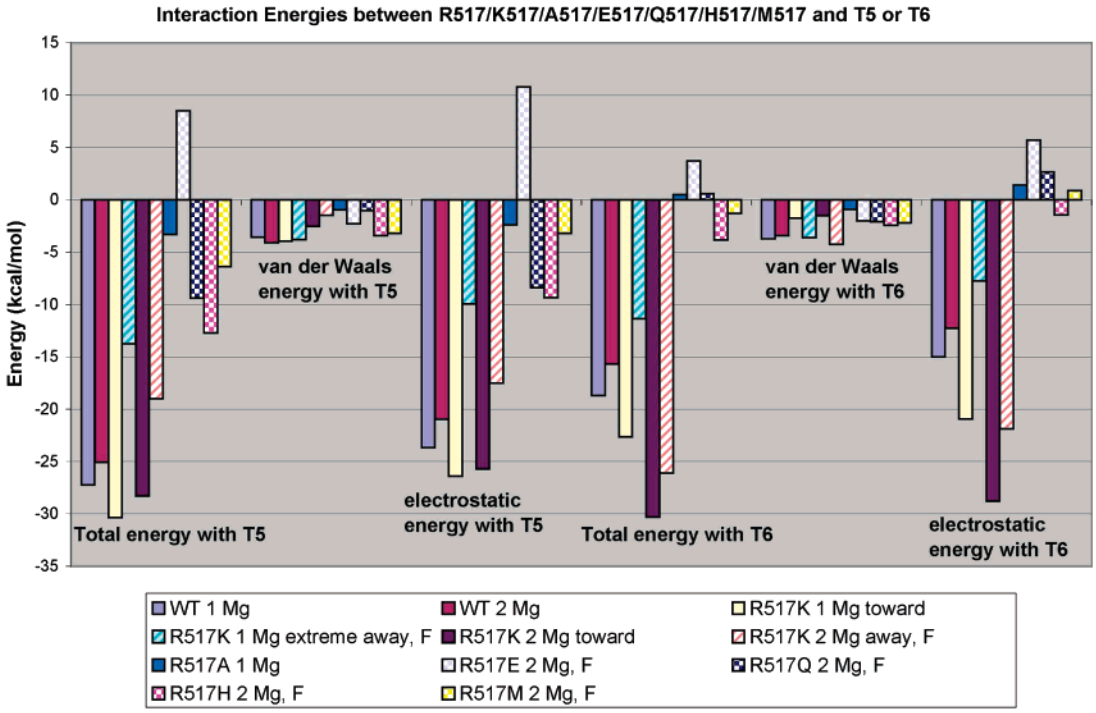

Figure 6. Interaction energies between Arg517, Lys517, Ala517, Glu517, Gln517, His517, or Met517 and T5 and T6, for equilibrated and final simulated systems. The equilibrated systems are wild-type pol λ ternary complexes with the nucleotide-binding ion (wild-type 1 Mg system) and both ions (wild-type 2 Mg system), equilibrated model of Arg517Lys pol λ mutant ternary complex with nucleotide-binding (R517K 1 Mg system) and both ions (R517K 2 Mg system), and equilibrated system of the ternary Arg517Ala pol λ complex (R517A 1 Mg system). In addition to these systems, calculations were also performed on the final state of several pol λ mutant systems (R517K 1 Mg, R517K 2 Mg, R517E 2 Mg, R517Q 2 Mg, R517H 2 Mg, and R517M 2 Mg systems). In the equilibrated systems of the Arg517Lys mutant complexes, Lys517 points toward the DNA, whereas in these systems after 20 ns of simulation time, Lys517 points away from the DNA. F symbolizes the final state of the simulation. A color key is provided.

Table 3. Average Trajectory Active Site Interatomic Distances for Pol λ Mutants[a]

distance (Å)	1K	2H	3Q	4K′	5E	6M	ternary (1XSN)
Nucleotidyl Transfer Distance							
dTTP (P_α) : *P*6 (O3′)	4.75	5.17	4.79	5.24	4.54	6.80	
Distance Between Magnesium Ions							
Mg^{2+}(A) : Mg^{2+}(B)	4.31	4.32	4.34		4.35	4.36	
Catalytic Magnesium Ion Coordination							
Mg^{2+}(A) : Asp427 ($O_{\delta1}$)	1.84	1.85	1.82		1.82	1.82	
Mg^{2+}(A) : Asp429 ($O_{\delta1}$)	1.83	1.81	1.84		1.85	1.85	
Mg^{2+}(A) : Asp490 ($O_{\delta1}$)	1.92	1.88	1.92		1.88	1.93	
Mg^{2+}(A) : Asp490 ($O_{\delta2}$)	1.89	1.92	1.88		1.93	1.90	
Mg^{2+}(A) : Wat1 (OH2)	2.04	2.11	2.10		2.08	2.13	
Mg^{2+}(A) : Wat2 (OH2)	1.99	1.98	1.98		1.98	1.98	
Nucleotide Magnesium Ion Coordination							
Mg^{2+}(B) : Asp427 ($O_{\delta2}$)	1.84	1.86	1.84	1.85	1.84	1.84	2.00
Mg^{2+}(B) : Asp429 ($O_{\delta2}$)	1.88	1.88	1.88	1.89	1.88	1.88	2.13
Mg^{2+}(B) : Wat3 (OH2)	2.05	2.04	2.07	2.05	2.08	2.06	2.15
Mg^{2+}(B) : dTTP ($O1_\alpha$)	1.89	1.91	1.89	1.90	1.89	1.89	1.98
Mg^{2+}(B) : dTTP ($O1_\beta$)	1.93	1.92	1.93	1.92	1.93	1.93	1.88
Mg^{2+}(B) : dTTP ($O3_\gamma$)	1.86	1.86	1.85	1.84	1.85	1.85	2.20

[a] Mg^{2+}(A), catalytic ion; Mg^{2+}(B), nucleotide-binding ion; dTTP, 2′-deoxythymidine 5′-triphosphate; *P*6, primer terminus; Wat1, Wat2, Wat3 water molecules.

tions of both wild-type and mutants of pol λ support this stabilizing role of Arg517 in the ternary state and demonstrate that critical interactions with the DNA are missing or altered when Lys, His, Glu, Gln, Met, or Ala are at position 517.

Our analyses also suggest that favorable electrostatic interactions between residue 517 and the DNA represent the driving force of DNA stability in pol λ. We observe a preference for interactions with T5 in both the wild-type and pol λ mutants, and this in turn results in more frequent hydrogen bonding between residue 517 and T5 than with T6. This tendency to interact with T5 more than T6 likely results from the shorter side-chain lengths of the other amino acids compared to that of Arg517. Although Lys517 displays the highest degree of similarity to Arg517 in terms of size and charge as well as the number of possible hydrogen bonds with the DNA (Table 2), it cannot reproduce Arg517's interaction strength because its flexible side chain prevents continuous hydrogen bonding with the DNA. Only the toward orientation of Lys517 promotes extensive hydrogen bonding with the DNA. As expected, Lys517's side-chain flexibility is somewhat reduced when both ions are bound (i.e., only the toward and away orientations are assumed during simulation 1K; Figure 4), and the range of DNA motion occurring in that simulation has greater similarity to the wild-type system. This is also suggested by the recent Arg517Lys pol λ crystal structure where the DNA is in the ternary conformation.[23]

The small His517 replacement has much less electrostatic stabilization with both bases than Arg517 and switches between two orientations, with only one permitting hydrogen bonding with the DNA. This explains transient DNA movement involving the template strand in the Arg517His pol λ mutant simulation.

The electrostatic repulsion of T6 by Ala517, Glu517 (which also repels T5), Gln517, and Met517 accounts for the significant DNA shifting toward the binary conformation that occurs during these simulations. Gln517's favorable electrostatic interactions with T5, however, partially compensate for the loss of interactions with T6 and limit the DNA transitioning that occurs during the Arg517Gln pol λ mutant simulation.

Taken together, we conclude that hydrogen bonding between residue 517 and the DNA helps restrain DNA template-strand movement, and particular orientations of residue 517 promote further hydrogen bonding with the DNA. Side-chain flexibility can disrupt these interactions, allowing the DNA template strand to become less stable in the ternary position. Thus, residue 517's interactions, including those with water and ions, which can vary in the active site, crucially affect protein/DNA contacts and can destabilize the DNA template.

Indeed, it was suggested that pol λ's frequent frameshift errors caused by single-base deletions occur through DNA template-strand slippage.[20] The X-ray crystal structures of pol λ/DNA deletion intermediates showed that one DNA template base is extrahelical upstream of the active site, whereas the DNA bases in the active site, namely the primer terminus basepair and the nascent basepair, are properly aligned.[20] Recently, on the basis of the experimental data and dynamics simulations, we proposed that DNA template-strand slippage may occur during dNTP-induced DNA repositioning.[23]

A consequence of this specific DNA motion in the 517 pol λ mutants is also the destabilization of active-site residues (i.e., Ile492, Tyr505, and Phe506), producing longer O3′−P_α distances, hence delaying the time and increasing energetic barriers of the chemical reaction. Steady hydrogen bonding between Arg488 and the primer terminus further constrains this catalytic distance. Other identified protein/DNA interactions (e.g., with Lys521, Arg538, and Lys544) may thus contribute to stabilizing/destabilizing the DNA in the ternary conformation through hydrogen bonding with the DNA template-strand backbone.

Interestingly, pol β's Arg283, which is analogous to pol λ's Arg517, plays an important role both in conformational transitions and in determining its fidelity.[27−31,40−43]Mutations of Arg283 to lysine or alanine cause decreases in pol β's fidelity by increasing its base-substitution and frameshift error rates.[27−31] The increased error rate of the Arg283Ala pol β mutant is partially explained by the more open conformation of the thumb subdomain in its X-ray crystal structure[27] and mutant simulation, where thumb opening also causes active-site residue destabilization.[40] Although pol λ relies on DNA template-strand repositioning to transition between its inactive and active conformations, whereas pol β utilizes large-scale subdomain motions, they share the general property that key residues are crucial to active-site organization and thereby affect fidelity profiles. Because pol λ's active site is less tight and specific than pol β's, frameshift errors can occur more easily when certain interactions are weakened by various internal and external factors.

In conclusion, our simulations reveal the importance of interactions between Arg517 and the DNA in pol λ and suggest that electrostatics, in particular, help maintain the DNA in the active position in pol λ's ternary state. Without Arg517, or with certain changes in ion and solvation near 517, significant DNA motions might occur; this DNA movement often reflects discrete changes in residue 517 orientation with respect to the DNA rather than continuous conformations. This DNA tendency to shift away from its active ternary position (Figure 2), as largely determined by the interactions between Arg517 and the DNA, appears to correlate with pol λ's frameshift errors. Thus, we suggest more generally that pol λ's architecture facilitates frameshift errors because of the large effect that small changes in the active site can have on the dynamics of the ternary pol λ complex. Ongoing studies will probe further into pol λ's intriguing structural features and error propensity.

Appendix

Geometric Characteristics. The movement of enzymes such as pol λ is not always accurately represented by a rmsd measure as a result of the magnitude and direction of domain motions. A previously developed approach to represent the rmsd data more accurately in such situations was employed to capture the motion of the DNA and subdomains in our pol λ simulations.[44] In this alternative methodology, we project the rmsd of the simulated structure on the line joining the geometric centers of the structure in the crystal binary and ternary conformations. As shown in Figure S10 (Supporting Information), this can be represented by a triangle where the crystal binary and ternary conformations form two vertices of the triangle and the simulated structure forms the third. The lengths of sides a and b of the triangle are given by the rmsd of the simulated structure relative to the crystal binary conformation and crystal ternary conformation, respectively, when the simulated structure and the corresponding crystal structure are superimposed with respect to all protein C_α atoms. The rmsd between the crystal binary and ternary conformations forms side c of the triangle and is held fixed. The shift distance, *h*, describes the displacement of the simulated structure in the direction perpendicular to the line joining the geometric centers of the structure in the crystal binary and ternary conformations. When *h* is constant, rmsd alone is a good measure of domain motions. When *h* is not constant, this is an appropriate methodology to use to represent domain motion toward the crystal states. The variable lengths L1 and L2 correspond to the projected rmsd of the simulated structure with respect to the crystal binary and ternary conformations, respectively.

Acknowledgment. We profited from discussions with Dr. Thomas Kunkel and his group at the NIH/NIEHS regarding their experimental work on pol λ and other polymerases. We especially appreciate the Kunkel group for providing us with some of their Arg517Lys and Arg517Ala pol λ mutant experimental data before publication. Research described in this article was supported in part by Philip Morris USA Inc. and Philip Morris International and by NSF grant MCB-0316771, NIH grant R01 ES012692, and the American Chemical Society's Petroleum Research Fund award (PRF #39115-AC4) to T.S. The computations are made possible by support for the SGI Altix 3700 by the National Center for Supercomputing Applications (NCSA) under grant MCA99S021, and by the NYU Chemistry Department resources under grant CHE-0420870. Molecular images were generated using the *INSIGHTII* package (Accelrys Inc., San Diego, CA).

Supporting Information Available: Appendix, supplemental Tables S1 and S2, and Figures S1−S10. This material is available free of charge via the Internet at http://pubs.acs.org.

JA077982T

(40) Yang, L.; Beard, W. A.; Wilson, S. H.; Broyde, S.; Schlick, T. *Biophys. J.* **2004**, *86*, 3392−3408
(41) Kirby, T. W.; DeRose, E. F.; Beard, W. A.; Wilson, S. H.; London, R. E. *Biochemistry* **2005**, *44*, 15230−15237.
(42) Radhakrishnan, R.; Arora, K.; Wang, Y.; Beard, W. A.; Wilson, S. H.; Schlick, T. *Biochemistry* **2006**, *45*, 15142−15156.
(43) Beard, W. A.; Wilson, S. H. *Chem. Rev.* **2006**, *106*, 361−382.
(44) Arora, K.; Schlick, T. *Biophys. J.* **2004**, *87*, 3088−3099.